



HAL
open science

X-rays energy measurements during the RFQ conditioning at the European Spallation Source

E. Laface, C.G. Maiano, R. Zeng, O. Piquet

► **To cite this version:**

E. Laface, C.G. Maiano, R. Zeng, O. Piquet. X-rays energy measurements during the RFQ conditioning at the European Spallation Source. IPAC 2022 - 13th International Particle Accelerator Conference, Jun 2022, Bangkok, Thailand. pp.TUPOTK030, 10.18429/JACoW-IPAC2022-TUPOTK030 . hal-03766024

HAL Id: hal-03766024

<https://hal.science/hal-03766024>

Submitted on 23 Jun 2023

HAL is a multi-disciplinary open access archive for the deposit and dissemination of scientific research documents, whether they are published or not. The documents may come from teaching and research institutions in France or abroad, or from public or private research centers.

L'archive ouverte pluridisciplinaire **HAL**, est destinée au dépôt et à la diffusion de documents scientifiques de niveau recherche, publiés ou non, émanant des établissements d'enseignement et de recherche français ou étrangers, des laboratoires publics ou privés.



Distributed under a Creative Commons Attribution 4.0 International License

X-RAYS ENERGY MEASUREMENTS DURING THE RFQ CONDITIONING AT THE EUROPEAN SPALLATION SOURCE

E. Laface*, C. G. Maiano, R. Zeng, European Spallation Source ERIC, Lund, Sweden
O. Piquet, CEA Paris-Saclay - DRF/Irfu/DACM, France

Abstract

The Radio Frequency Quadrupole (RFQ) was conditioned at the European Spallation Source during spring 2021. We used part of the conditioning time to estimate the accelerating potential within the RFQ analyzing the x-rays bremsstrahlung radiation emitted by the electrons released and accelerated in the RFQ. The results of these measurements are in good agreement with the theoretical prediction.

INTRODUCTION

The Radio Frequency Quadrupole, [1] section 3.2 and [2], is an accelerating, focusing and bunching structure located after the Ion Source and Low Energy Beam Transport at the European Spallation Source in Lund, Sweden. This structure has the goal of accelerating the 62.5 mA of proton beam from 75 keV to 3.6 MeV at a frequency of 352.21 MHz with a repetition rate of 14 Hz for a pulse of 2.86 ms. In order to achieve this goal, the RFQ needs several weeks (in our case eight) of conditioning, where the power, the repetition rate and the length of the pulse are gradually increased up to the nominal level. The conditioning phase removes the residual contaminants deposited on the surface, as well as surface imperfections, making the device stable in terms of operations.

A side effect of the RFQ powering is that some electrons are generated and accelerated within the RFQ itself and, when those electrons hit the surface they release the energy as x-rays that can be measured outside the RFQ structure. The distribution of energies among the electrons follows the spectrum of bremsstrahlung, and in particular the maximum reachable energy (the asymptotic behaviour) is expected to be the potential produced within the RFQ. This gives a method to measure the potential produced in the RFQ for each applied power [3–5].

THE X-RAYS DETECTOR

The x-rays measurements were performed using CdTe detector from Amptek: Model XR-100-CdTe is a high performance x-rays detector, pre-amplifier, and cooler system using a $5 \times 5 \times 1 \text{ mm}^3$ Cadmium Telluride (CdTe) diode detector mounted on a two-stage thermoelectric cooler. Cadmium Telluride (CdTe) crystal is the sensor material for direct conversion of the x-rays radiation [6]. This high-Z semiconductor material (Cd with $Z=48$, Te with $Z=52$) provides excellent stopping power and thus high efficiency in the desired energy range (see Fig. 1).

* emanuele.laface@ess.eu

The detector and Digital Pulse processor, (Fig. 2) were installed on a flange outside the fourth slot of the fifth RFQ module at a distance of 3.03 m from the beginning of the RFQ (Fig. 3).

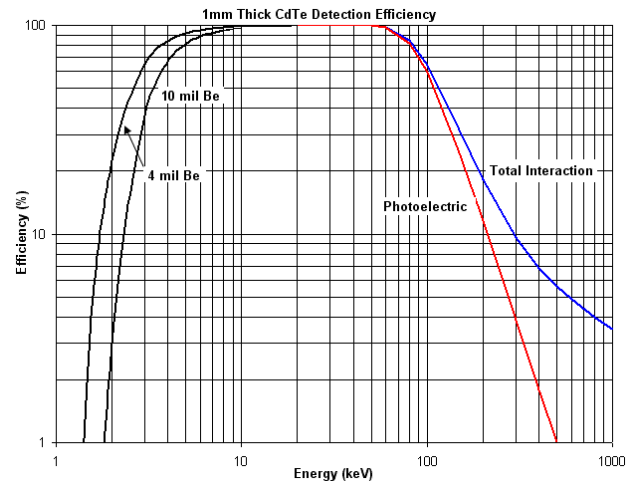


Figure 1: Detector efficiency (1 mm thick crystal).

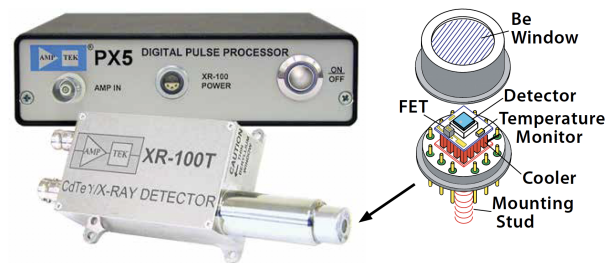


Figure 2: Detector.

After some tests of setup it was decided to avoid the use of a shielding liner for the installation of the x-ray detector because the copper of the RFQ and the stainless steel of the flange was sufficient to shield the low energy x-rays avoiding the saturation of the detector.

Calibration

Before starting to acquire the measurements we did a calibration of the detector, using isotopes with lines in the energy region of interest, which is from 0 to 120 keV. The selected sources for the calibration were:

- ^{241}Am with lines at 13.81, 17.70, 20.70, 26.34 and 59.54 keV as in Fig. 4

Content from this work may be used under the terms of the CC BY 4.0 licence (© 2022). Any distribution of this work must maintain attribution to the author(s), title of the work, publisher, and DOI



Figure 3: Detector installed on the RFQ flange.

- ^{152}Eu with lines at 39.52, 45.41 and 121.78 keV as in Fig. 5

The linear function between channels and energy is obtained with a best fit between the calibrated points (Fig. 6). The residual error of the fit, that is of 0.3 keV, is used as error in the energy measurement of the instrument.

Configuration

The detector configuration was selected starting from Amptek general guideline, fine tuned for our specific case. Parameters like detector voltage and and peak time were unchanged, since the energy resolution had been already optimized at the vendor: nominal: 25 mm² crystal shows < 1.5keV FWHM at ^{57}Co 122 keV line. The total number of channels of 2048 and the gain of 12 were chosen to focus on the energy detection window from 0 to slightly above 120 keV (the maximum energy peak visible in the spectrum was ^{152}Eu line at 121.78 keV). No pile-up rejection mode (PUR) option was activated since the rate of events was sufficiently low: no dead time was measured at any power level.

MEASUREMENTS AND ANALYSIS

The x-rays spectrum was acquired for each value of the forward power from 450 to 800 kW with steps of 50 kW. The pulse that was sent to the RFQ was, for all the acquisitions, the nominal one: 2.86 ms of flat top pulse with a repetition rate of 14 Hz. For each set-point the data were acquired for a time long enough to see a clear signal over the noise background. This means that the time of acquisition at low power was much longer than the time of acquisition at high power because the rate of detected x-rays was lower at lower power. For this reason, the counts per channel are normalized with time in the data analysis, such that the comparison is homogeneous. A background measurement, that is at zero power in the RFQ, was acquired during a shutdown, normalized to the acquisition time and subtracted from the power measurements. The measured background is due to

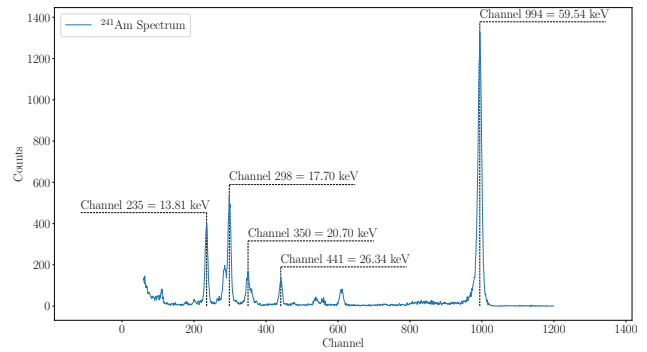


Figure 4: Calibration with ^{241}Am source.

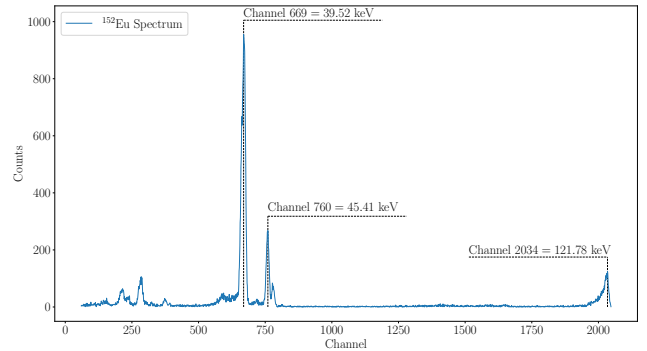


Figure 5: Calibration with ^{152}Eu source.

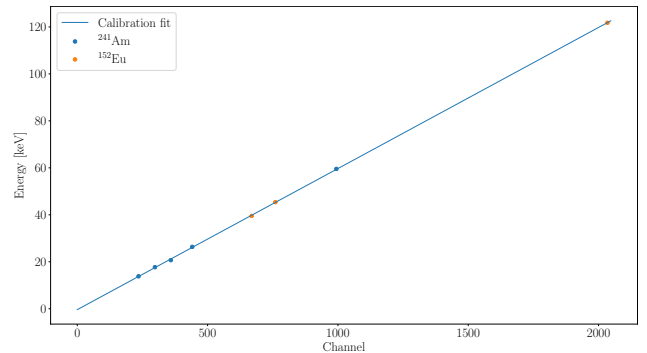


Figure 6: Calibration fit.

natural radioactivity of the materials surrounding the detector. Isotopes like ^{232}Th and ^{40}K are, with high probability, contained in the concrete walls and Compton continuum extends to low energy region where our ROI sits.

The acquisitions showed a clear bremsstrahlung pattern in the performed measurement, as an example we show the acquisition spectrum at 650 kW in Fig. 7.

The spectrum was analyzed to identify the limit in energy of the electrons. This limit is, in first approximation, when the linear component of the spectrum intercept the zero of the counts. The first step is to identify the linear region applying a movable average with a windows of 20 channels. The size of this window was chosen after several test with different sizes in order to reduce the noise maintaining, at the same time, the underlying physics. The linear fit is then performed on the most linear region (the largest identified that minimize the quadratic error between the linear fit and the data). Finally the value of the zero intersection is evaluated

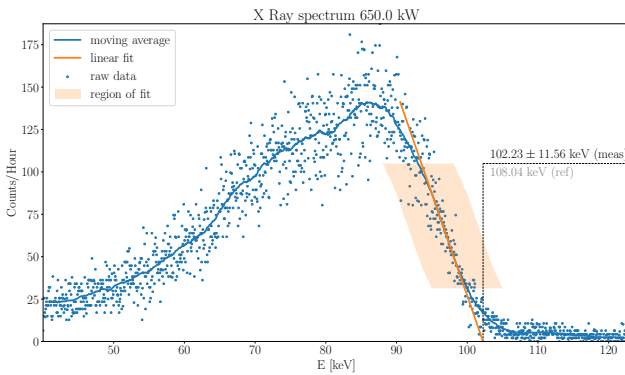


Figure 7: Example of a spectrum: 650 kW of inward power at 14 Hz, 2.86 ms. The error reported here in the measurement is only the residual of the linear fit, the full error must account also the instrument error from the calibration procedure as previously described. The background was subtracted from a background measurement done when the power in the RFQ was zero. The residual background from natural activity and cosmic rays is visible as the counts after the bremsstrahlung region.

Table 1: Energy vs. Power in the RFQ. Theoretical estimation and values measured from the bremsstrahlung electrons. The point at 500 kW was rejected because the power was changed during the measurement and the final value cannot be estimated.

Power [kW]	Theoretical [keV]	Measured [keV]
450 ± 4.18	86.5	89.27 ± 1.74
550 ± 6.87	95.63	95.51 ± 3.51
600 ± 6.90	99.89	99.57 ± 6.56
650 ± 8.45	103.96	102.33 ± 11.86
700 ± 10.71	107.81	106.67 ± 7.12
750 ± 9.00	111.67	109.14 ± 9.81
800 ± 8.40	115.33	112.26 ± 28.62

as the maximum energy of the bremsstrahlung electrons, with the error estimated as the square root of the residuals.

The measured value was compared with the theoretical estimation based on the model of the RFQ. The values are reported in Table 1. The point at 500 kW was rejected because we discovered during the analysis that the power in the RFQ was not kept constant during the measurement, generating a spectrum that was not possible to use for the linear extrapolation.

The errors reported in Table 1 for the measured values are the square root of the residuals of the linear fit combined with the error of the detector. The errors on the power readings are the errors between the set-point and the real value of power applied to the RFQ. The overview of the measurements with errors and the theoretical value is in Fig. 8 where, for comparison, was it added also the value of the voltage measured in the power meters (PK) installed in the RFQ scaled at the position of the x-ray detector. The error on the PK signal is the nominal power meter calibration error, around 0.2 dB, that corresponds to 5%.

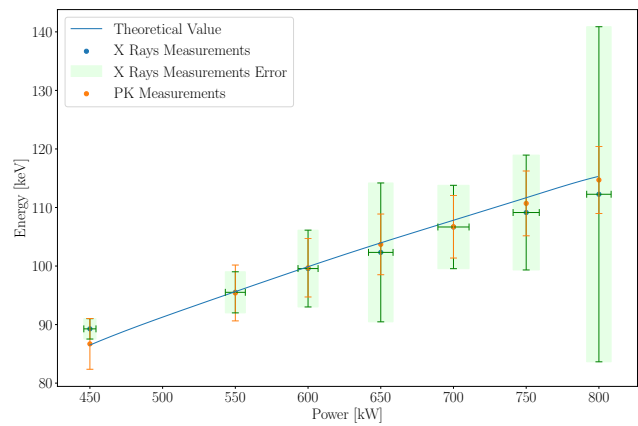


Figure 8: Energy vs. power plot. The solid line is the theoretical value, the blue dots are the x-rays measurements with the error bars in green; the orange dots are the measured voltage in the RFQ from the PKs, reported with their errors for comparison.

CONCLUSIONS

The analysis of the bremsstrahlung x-rays produced by the electrons in a RF device such as the RFQ can be exploited to estimate the maximum accelerating field generated within the device. We proved that the obtained values from the measurements at different powers, from 450 to 800 kW in the RFQ, are in good agreement with the theoretical estimation from the model and from the readings obtained by the power meter PKs. The main source of errors in the analysis is the noise in the fit that can be reduced with long acquisition time.

We also proved that the ESS RFQ is producing an accelerating field according to the design and it is ready for the next phase of operations that is the beam commissioning. A similar technique of x-ray analysis was applied to the superconducting cavities at the ESS, using different kind of detectors, and the results are available on paper TUPOTK027 in this conference [7].

REFERENCES

- [1] R. Garoby, A. Vergara, H. Danared, I. Alonso, E. Bargallo, B. Cheymol, C. Darve, M. Eshraqi, H. Hassanzadegan, A. Jansson *et al.*, “The European spallation source design,” *Physica Scripta*, vol. 93, no. 1, p. 014001, 2017. doi:10.1088/1402-4896/aa9bff
- [2] O. Piquet *et al.*, “ESS RFQ: Construction Status and Power Couplers Qualification”, in *Proc. IPAC’19*, Melbourne, Australia, May 2019, pp. 855–857. doi:10.18429/JACoW-IPAC2019-MOPTS008
- [3] C. P. Bailey *et al.*, “First Results from the ISIS RFQ Test Stand”, in *Proc. EPAC’00*, Vienna, Austria, Jun. 2000, paper THP4A05, pp. 833-835.
- [4] R. Ferdinand *et al.*, “SPIRAL2 RFQ Prototype – First Results”, in *Proc. EPAC’06*, Edinburgh, UK, Jun. 2006, paper MOPCH103, pp. 282–284.
- [5] P. P. Schneider *et al.*, “First Experiments at the CW-Operated RFQ for Intense Proton Beams”, in *Proc. LINAC’16*, East

Lansing, MI, USA, Sep. 2016, pp. 394–397. doi:10.18429/JACoW-LINAC2016-TUOP05

cdte-cadmium-telluride-detector-efficiency-application-note/.

[6] A. I. Robert Redus, “Efficiency of XR-100T-CdTe Detectors Application Note (AN-CdTe-001 Rev. 1)”. 2021. <https://www.amptek.com/internal-products/xr-100t->

[7] C. G. Maiano *et al.*, “Field Emission Measurements at ESS Lund Test Stand”, presented at the IPAC’22, Bangkok, Thailand, Jun. 2022, paper TUP0TK027, this conference.